

# 2D modeling for acoustic waves in solids with frictional cracks

S. DELRUE<sup>a</sup>, V. ALESHIN<sup>b</sup>

a. Wave Propagation and Signal Processing Research Group,  
KU Leuven Kulak, Kortrijk, Belgium,  
Steven.Delrue@kuleuven.be

b. Joint International Laboratory LICS/LEMAC,  
Institute of Electronics, Microelectronics and Nanotechnologies,  
UMR CNRS 8520, Villeneuve d'Ascq, France,  
Vladislav.Aleshin@iemn.univ-lille1.fr

## Abstract :

*Contact acoustic nonlinearity underlies modern non-destructive testing methods that use nonlinear ultrasound to detect cracks, delaminations, debonding, defects in weldings, imperfect gluing, etc. Since the nonlinear response of a sample highly depends on the actual configuration of internal contacts (called cracks for brevity), there is a high need for realistic numerical models in order to be able to fully understand the microscopic behavior of contact defects and to predict their macroscopic nonlinear response. In this communication, we present a numerical toolbox for modeling vibrations or acoustic wave propagation in solids containing cracks of known geometry. The numerical tool consists of two components: a unit for solving the elasticity equations in the bulk volume and a unit that provides appropriate boundary conditions to be imposed at the internal crack boundaries in the material. The full model allows the user to calculate the nonlinear time-dependent distributions of stress, strain, displacement, etc., in a sample in response to an ultrasonic excitation, and to compare the results to actual measurements. The final objective would be to estimate geometric and physical parameters of defects using this comparison.*

## Keywords :

Contact Acoustic Nonlinearity, Crack, Friction, Crack-Wave Interaction, COMSOL Multiphysics

## 1 Introduction

For many years, acoustic waves have been extensively used for damage detection and characterization. An important class of acoustic wave based techniques relies on the reflection, transmission or scattering of the excited waves at defects [1]. Unfortunately, these techniques are not capable of accurately detecting contact-type defects, such as cracks, delaminations, debonding, imperfect gluing, etc. However, these defects can generate high levels of nonlinearity, often referred to as Contact Acoustic Nonlinearity (CAN) [2], leading the way for Nonlinear Elastic Wave Spectroscopy (NEWS) techniques to be used for their detection and localization [3, 4]. The nonlinear features generated by interactions of the acoustic

waves with the contact-like defects are mainly induced by clapping and frictional behavior of the defects. Clapping is related to the normal wave-defect interaction, causing the contact interface to continuously switch between open and closed states. In the open state both interfaces of the contact can move freely, while in the closed state there exists interaction. This results in a bimodal (nonlinear) behavior of the elastic moduli depending on the state of the contact. On the other hand, friction is related to the tangential wave-crack interaction and results in a nonlinear tangential force-displacement relationship [5, 6]. Contact acoustic nonlinearity is usually much stronger than other types of acoustic nonlinearity, such as material or geometric nonlinearity.

The main bottleneck in using nonlinear techniques for the detection contact-like defects is an incomplete understanding of the underlying microscopic mechanisms. The development and implementation of realistic constitutive models that allow a better understanding and analysis of the nonlinear behavior of these defects is therefore necessary. In-depth analytical and numerical studies would lead to optimization of the existing experimental techniques for defect detection and to the development of new methods and approaches. On the other hand, a dedicated comparison of experimentally obtained nonlinear indicators with the results obtained by dedicated numerical modeling, would lead to a full characterization of the detected defects, allowing to make a prediction about the lifetime or serviceability of the tested samples and structures.

Over the past decades, several models have been proposed to explain nonlinear crack-wave interactions [6]. These models can be divided into two classes: the phenomenological models and the physical models. The first class of models tries to simulate the desired nonlinear behavior by means of simple (or more complex) stress-strain relations. These models can only be used for imitating contact nonlinearity in a qualitative way and not for explaining its physical behavior. The physical models, on the other hand, are more realistic, as they assume that there are physical mechanisms responsible for the nonlinear behavior of the defects. The model proposed here belongs to this class of models and is based on the physics of normal and tangential interactions instead of artificial assumptions. The model contains two components: a unit for solving the elasticity equations in the bulk volume, and a unit that provides the appropriate boundary conditions to be imposed at the internal boundary corresponding to the contact. The solid mechanics unit can be programmed using an available finite element software that accepts internal boundaries and user-supplied boundary conditions. We have used COMSOL Multiphysics<sup>®</sup> [7], whose features provide an interface to an external crack model programmed in MATLAB<sup>®</sup> [8].

In this communication, we explain the numerical model for wave-crack interaction was developed and implemented. We also present an illustrative example of wave propagation in a sample of known geometry and quantitatively illustrate its nonlinear behavior. The obtained results will prove the potential of the developed model that may be of interest for researchers working in experimental non-destructive testing, nonlinear acoustics, or dealing with vibrations of loaded contacts, nonlinear metamaterials, imaging techniques including nonlinear vibrometry, thermography, etc.

## 2 Modeling of Contact Acoustic Nonlinearity (CAN)

The description of CAN often requires the junction of two classical disciplines: acoustics and contact mechanics. The developed numerical tool also contains two components: the constitutive crack model and the elastic wave propagation model. The crack model is created using physics-based theoretical considerations. The presence of cracks invokes two major mechanisms of nonlinearity: (1) an asymmetric reaction of the crack on normal compression/tension, and (2) friction-induced hysteresis activated by

shearing action. On the other hand, an internal contact can evolve in one of several regimes, such as contact loss, stick, and sliding. The crack model has to take into account these phenomena to provide the nonlinear load-displacement relationships for any value of the drive parameters. As such, the model is based on the following essential features:

- the considered contact model includes friction based on the Coulomb friction law,
- the internal contact/crack surfaces have a nontrivial topography (e.g. roughness),
- the normal load-displacement dependency for rough surfaces requires some information on roughness statistics, or otherwise it can be measured directly for an engineered contact,
- the tangential interactions appear during shift; rolling and torsion as movement types are not considered,
- plasticity and adhesion are neglected.

The introduction of roughness is important, as it allows to provide contact load-displacement solutions in explicit form, which is not possible in case of plane surfaces. Indeed, for plane contact faces, the Coulomb friction law only defines in which state (contact loss, stick or sliding) the system evolves at some given load. Displacements can only be calculated using an implicit procedure that redistributes strains and stresses in the whole sample trying to match the sliding condition. In the following subsections, we will explain how the introduction of a nontrivial topography helps avoiding this difficulty and we will briefly discuss the implementation of the two components in the numerical tool.

## 2.1 Constitutive crack model

The approach to calculate the desired physics-based relationships between normal and tangential loads  $N$  and  $T$  (i.e. forces per unit of nominal contact area), and normal and tangential displacements  $a$  and  $b$  requires the introduction of an intermediate scale, or in other words, a mesoscopic cell. On one hand, the size of this cell is considerably less than both the crack size and the wavelength, so that the calculated macroscopic elastic fields are approximately uniform within each cell. On the other hand, the cell size is much greater than the scale of roughness. The concept of the mesoscopic cell is illustrated in Fig. 1. The top part represents a real crack in a sample. The middle figure illustrates how this crack is approximated by a number of mesoscopic cells. The bottom part shows the geometry of the auxiliary problem to be solved in each mesoscopic cell for determining the load-displacement relationship.

The contact in a mesoscopic cell can evolve in one of three regimes: contact loss ( $N = T = 0$ ), total sliding ( $|T| = \mu N$ , with  $\mu$  the friction coefficient) and partial slip ( $|T| < \mu N$ ). The latter case occurs when both stick and slip areas are present in the contact zone and is only possible due to the presence of surface roughness. In case of perfectly smooth surfaces, the condition  $|T| < \mu N$  actually corresponds to the state of stick in accordance to Coulomb's law of friction. The partial slip regime is successfully dealt with by using the previously developed Method of Memory Diagrams [9]. In this method, the required explicit relation between loads and displacements is constructed with the help of an internal system function (memory diagram function) that contains all memory information present in the system. The memory diagram function has to be maintained at each mesoscopic cell on the crack interface and evolves in accordance to a number of prescribed rules and offers the possibility to calculate hysteretic tangential reaction curves as a function of displacement histories  $a(t)$  and  $b(t)$ . However, to do so, MMD

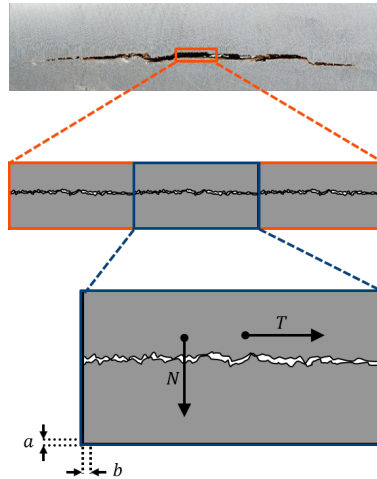


Figure 1: Illustration of the concept of the mesoscopic cell. The top part represents a real crack in a sample. The middle part illustrates the approximation of the crack by a number of mesoscopic cells. The bottom part shows one mesoscopic cell in which normal and tangential loads ( $N$  and  $T$ ) and displacements ( $a$  and  $b$ ) are defined.

requires the knowledge of the normal contact reaction  $N = N(a)$  for the system under study. Based on some theoretical [9] and experimental [10] arguments, the normal reaction curve  $N(a)$  is considered to have a quadratic dependency:

$$N(a) = C^2 a^2, \quad (a \geq 0), \quad (1)$$

where  $C = 6 \times 10^{10} \text{ Pa}^{1/2} \text{ m}^{-1}$ . This approximation only works for small  $a$  (i.e. weak acoustic strains).

This displacement-driven solution obtained using MMD can be easily extended onto the two other contact regimes (contact loss and total sliding), and can finally be computed for any arbitrary combination of normal and tangential displacement values and their time dependencies. For this, the following approach is used. First, the tangential displacement  $b$  is presented as a sum of two components:

$$b = b_0 + \tilde{b}, \quad (2)$$

where  $b_0$  corresponds to the displacement achieved in the total sliding regime, and  $\tilde{b}$  is a component that reflects partial slip and the ability of asperities to recede under tangential load. Then, a solution for each of the three contact regimes can be defined:

- Contact loss occurs when  $a \leq 0$ . In this case, no contact interaction is present, meaning that  $N = T = 0$ . As a result, asperities remain unstrained at this moment, meaning that  $\tilde{b} = 0$ , and hence  $b_0 = b$ . These modifications will guarantee correct evolution of the memory diagram function once the crack faces will ever get in contact.
- Partial slip occurs when  $a > 0$  and  $|\tilde{b}| < \theta \mu a$ . The second identification criterion actually corresponds to Coulomb's condition for stick regimes, which, in this case, is written for displacements instead of the more traditional condition written for forces. The parameter  $\theta$  is a material constant that for axisymmetric profiles depends on Poisson's ratio:

$$\theta = \frac{2 - \nu}{2(1 - \nu)}. \quad (3)$$

For non-axisymmetric geometries, the value of  $\theta$  can differ from Eq. (3). In the partial slip case, the total sliding contribution  $b_0$  remains unchanged and hence  $\tilde{b} = b - b_0$ . Using this new value for  $\tilde{b}$  as an argument in the MMD algorithm, the tangential load  $T$  can be calculated. The magnitude of the normal load  $N$  is calculated using equation (1).

- Total sliding occurs when  $a > 0$  and  $|\tilde{b}| \geq \theta\mu a$ . Similar to the partial slip case, the second identification criterion corresponds to Coulomb's condition for slip regimes, again written for displacements. In this case, the tangential load is determined in accordance to the Coulomb friction law,  $T = \pm\mu N$ , where the magnitude of  $N$  is again calculated using equation (1). To guarantee correct evolution of the memory diagram function during the next time steps, we also set  $\tilde{b} = \pm\theta\mu a$ , as this is the maximum possible tangential displacement corresponding to elastic deformation of asperities, and, as a result,  $b_0 = b - \tilde{b}$ .

Finally, the calculated link between contact loads and displacements is used as an internal boundary condition defined at the crack boundaries in the elastic wave propagation model.

## 2.2 Elastic wave propagation model

The elastic wave propagation model is implemented in the commercially available, finite element software package COMSOL Multiphysics<sup>®</sup>[7]. Cracks are introduced on internal boundaries using the 'thin elastic layer' boundary condition, which decouples the displacements between the two sides of the boundary and connects them by introducing normal and tangential forces per unit area ( $F_n$  and  $F_t$ ) with equal size, but opposite directions. These forces need to be included by the user and can be expressed as an external algorithm written in MATLAB<sup>®</sup> and connected to COMSOL<sup>®</sup> using the LiveLink<sup>™</sup> for MATLAB<sup>®</sup> [8].

The connection between COMSOL<sup>®</sup> and MATLAB<sup>®</sup> ensures a simple and explicit procedure of data exchange between the crack model and the elastic wave propagation model. By implementing the above described constitutive crack model in MATLAB<sup>®</sup>, it is possible to provide a direct link between the calculated load-displacement relationships ( $N(a)$  and  $T(a, b)$ ) from the crack model and the forces needed at the internal crack boundaries in the elastic wave propagation model ( $F_n$  and  $F_t$ ). In particular, the following relations can be defined:

$$F_n = -N(a) + N_0, \quad (4)$$

$$F_t = T(a, b). \quad (5)$$

The terms  $N(a)$  and  $T(a, b)$  are the solutions from the constitutive crack model, which allow to calculate the contact forces for any value of the normal and tangential displacements  $a$  and  $b$ , and depending on the current contact state (contact loss, full sliding or partial slip). The negative sign in front of  $N(a)$  is due to the different conventions used in contact mechanics (i.e. the crack model) and in the solid mechanics unit of COMSOL<sup>®</sup> (i.e. the elastic wave propagation model). In contact mechanics, a positive normal load  $N$  is considered as the load used to press the contacting faces against each other, while in COMSOL<sup>®</sup>, the positive normal force  $F_n$  corresponds to the reaction force due to this pressure. The term  $N_0$  in Eq. (4) is assumed to be a normal pre-load that closes the crack ( $N_0 \geq 0$ ). When differing from zero,  $N_0$  for instance corresponds to some weight added to the structure, an external load or a residual stress due to plasticity.

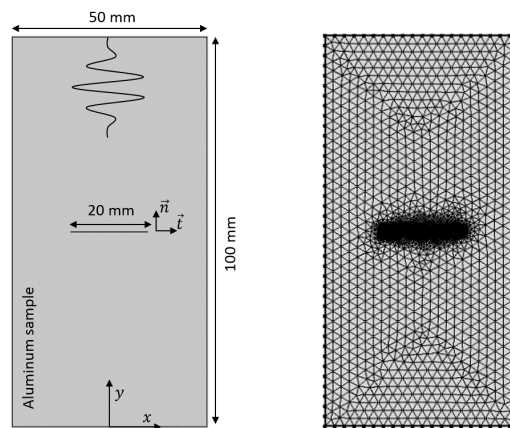


Figure 2: Illustration of the geometry implemented in COMSOL<sup>®</sup>, together with the generated mesh. The geometry consists of a rectangular aluminum domain with a crack of finite extent positioned in the center of the aluminum domain. The geometry was meshed with triangular mesh elements. Smaller mesh elements were generated in the region of the crack, in order to obtain a stable solution.

### 3 Illustrative example

In order to illustrate the potential of the above described model, an illustrative example of a shear wave propagating in a 2D aluminum crack sample is studied. The model geometry consists of a rectangular aluminum domain of 50 mm width and 100 mm height, as illustrated in Fig. 2. The aluminum sample has a density  $\rho = 2700 \text{ kg/m}^3$ , Young's modulus  $E = 70 \text{ GPa}$ , and Poisson's ratio  $\nu = 0.33$ . A crack with a length of 20 mm is positioned in the center of the sample. On the top boundary of the sample, a continuous shear wave excitation with a frequency of  $f = 100 \text{ kHz}$  and amplitude  $A = 100 \text{ nm}$  is defined. The other boundaries of the sample are considered to be low reflecting boundaries. At the internal crack boundaries, a thin elastic layer boundary condition is specified, according to the above description. The friction coefficient  $\mu$  needed in the crack model is set equal to one.

As illustrated in Fig. 2, the full geometry is meshed using quadratic triangular elements with a maximum size of approximately 2.6 mm. Smaller mesh elements are generated in the region of the crack, since the crack model requires a small spatial discretization size in order to obtain a stable and accurate solution. here a fixed number of 150 mesh elements at the internal crack boundary is adopted. The wave propagation problem is solved using the implicit generalized alpha time-dependent solver in COMSOL<sup>®</sup>. The get accurate solutions, the time step for this particular simulation is  $\Delta t = 25 \text{ ns}$ , corresponding to 400 time steps per wave cycle.

In the current example, we particularly focus on the tangential interaction between the crack faces (i.e. partial slip and full sliding), in order to reveal the nonlinear hysteretic tangential behavior. To make sure that the contacting faces are always in contact (i.e. no contact-loss regime), a pre-load  $N_0 > 0$  is introduced in the contact laws. The larger the pre-load, the more difficult it becomes to open the crack and initiate clapping. If there is no or only a small pre-load, it is expected that the crack will switch between one of the three contact states (contact loss, total sliding or partial slip) when the ultrasonic wave starts interacting with it. Increasing the pre-load, however, will result in only closed states (total sliding or partial slip) as the amplitude of the interacting ultrasonic wave is too low to overcome the defect activation threshold for clapping that is induced by the pre-loading. If the pre-load is increased even more, only partial slip will occur.

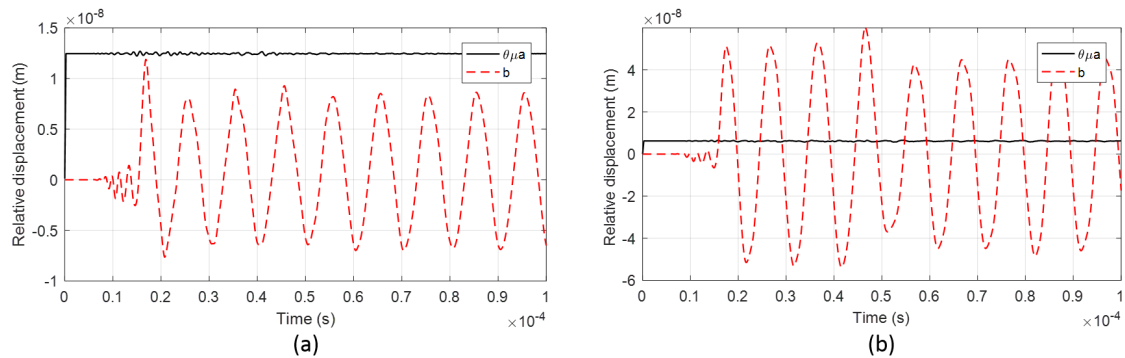


Figure 3: Calculated normal and tangential relative displacements,  $a$  and  $b$ , at the central point on the crack interface in case of a shear wave excitation at 100 kHz with amplitude  $A = 100$  nm. (a) Case with pre-loading  $N_0 = 0.36$  MPa, (b) Case with pre-loading  $N_0 = 0.09$  MPa.

### 3.1 Linear wave-crack interaction

The interaction of the excited ultrasonic shear wave with the crack is illustrated for two cases with different amounts of pre-loading. The first case corresponds to a pre-loading  $N_0 = 0.36$  MPa, while the second case corresponds to a pre-loading  $N_0 = 0.09$  MPa.

The effect of the pre-loading is illustrated in Fig. 3 where the time evolution of the calculated normal and tangential relative displacements,  $a$  and  $b$ , at the central point on the crack interface is plotted. Figure (a) corresponds to the case with the largest pre-loading. In both situations, application of the normal pre-loading closes the crack and results in the appearance of a positive normal displacement  $a$  due to the fact that asperities in contact can recede under load. The larger the pre-load, the higher the value of  $a$ . In the first case, the induced normal displacement  $a$  is large enough such that the tangential displacement  $b$  is always smaller than  $\theta\mu a$ , which means that the central position of the crack will be in a state of partial slip. It can be verified (not shown here) that this will also be the case for other positions on the crack. In the second case, where there is less pre-loading, the tangential displacement  $b$  often exceeds  $\theta\mu a$ , which means that the central position of the crack will switch between the partial slip and full sliding regimes. Also in this case, it can be verified (not shown here) that other positions on the crack will behave in the same way.

Fig. 4 shows snapshots of the calculated total displacement in the cracked aluminum samples, illustrating the (linear) interaction of the ultrasonic shear wave with the crack. In figure (a), a snapshot at  $t = 10 \mu\text{s}$  is shown. At this particular instant in time the wave is propagating through the sample in the direction of the crack, but has not reached the crack yet. In figures (b) and (c), a snapshot at  $t = 18 \mu\text{s}$  is shown for both the pre-loaded cases. The first situation (large pre-loading) was defined as the case in which only partial slip occurs. In this case, both crack faces stick to each other and move perfectly together in both normal and tangential direction. Hence, the crack does not influence the (linear) wave propagation. However, we will show later, that even though no linear interaction is observed, there will still be some nonlinear interaction due to the receding of crack asperities. The second situation (smaller pre-loading) was defined as the case in which the crack switches between the states of partial slip and full sliding. In case of full sliding, the tangential displacement of the contacting faces differs relative to each other. This causes a discontinuity in the tangential displacement in the sample at the position of the crack, which clearly influences the (linear) wave propagation.

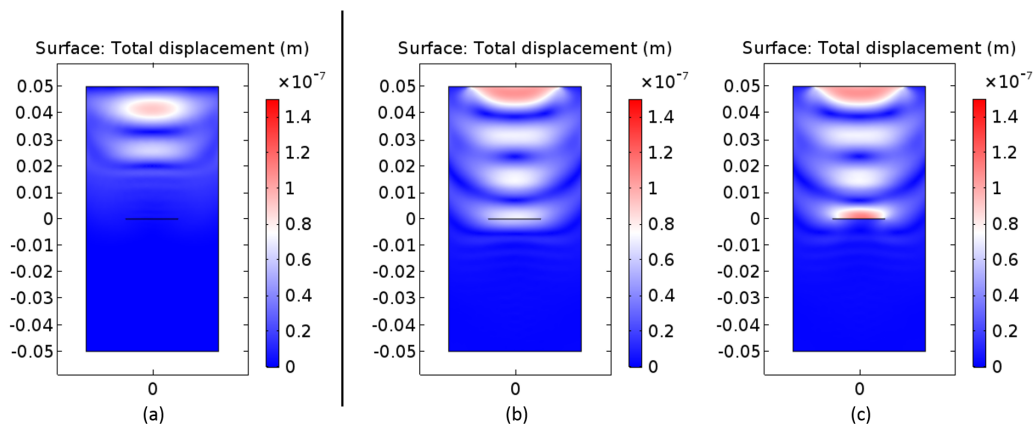


Figure 4: Snapshots of the calculated total displacement in the cracked aluminum sample. (a)  $t = 10 \mu\text{s}$ : Shear wave has not reached the crack yet. (b)  $t = 18 \mu\text{s}$  and  $N_0 = 0.36 \text{ MPa}$ : Shear wave propagation is not influenced by the crack. (c)  $t = 18 \mu\text{s}$  and  $N_0 = 0.09 \text{ MPa}$ : Shear wave propagation is highly influenced by the crack.

## 3.2 Nonlinear hysteretic behavior

The nonlinear hysteretic behavior that results from the interaction of the ultrasonic shear wave with the crack, is, for both pre-loading cases, illustrated by the hysteretic tangential reaction curves in Fig. 5. These curves show the evolution of the tangential stress  $\sigma_{xy}$  at the central point of the crack as a function of the relative tangential displacement  $b$  between the crack faces. Figure (a) corresponds to the case with large pre-loading ( $N_0 = 0.36 \text{ MPa}$ ), where only partial slip is observed, and therefore depicts the tangential, hysteretic deformations that the asperities undergo during wave-crack interaction. Figure (b) corresponds to the case with less pre-loading ( $N_0 = 0.09 \text{ MPa}$ ), where the crack switches between the partial slip and total sliding states. The switching between the two states is clearly visible in the tangential reaction curve. At the start of the wave-crack interaction, the relative tangential displacement is still small (i.e. less than approximately  $10 \mu\text{m}$ ), such that the crack is in a state of partial slip. This is evidenced by the central closed loop in the reaction curve, similar to the closed loops observed in figure (a). However, at a certain moment in time, the relative tangential displacement exceeds the Coulomb law threshold for total sliding and the crack faces start to slide. During this sliding motion, the tangential stress can never exceed the normal contact stress, which is mainly induced by the pre-loading and slightly influenced by the ultrasonic wave propagation. Hence, the tangential stress should be approximately equal to  $N_0 = 0.09 \text{ MPa}$ , which corresponds to the horizontal sections in the hysteresis curve. Once the tangential displacement drops again below the Coulomb threshold for total sliding, the tangential stress starts to change again, which corresponds to the vertical sections in the hysteresis curve.

## 4 Conclusion

This paper contains the description of a numerical tool created for modeling acoustic wave propagation in materials containing internal frictional contacts. The tool consists of two components: a constitutive crack model and a unit that solves the elasticity equations in the bulk volume. The theoretical crack model takes into account non-trivial topography (e.g. roughness) of internal contacts. For these topographies, there exists a contact regime called partial slip where some points of the contact area slide



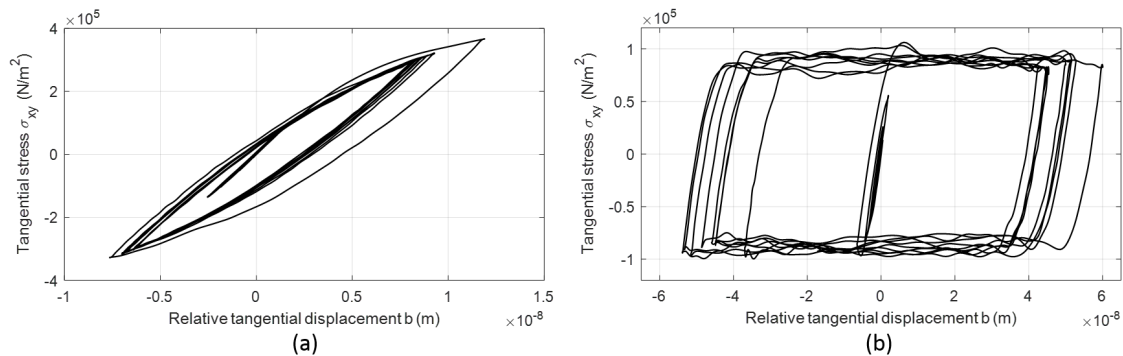


Figure 5: Tangential reaction curves: (a) Hysteretic curve in case of partial slip (pre-load  $N_0 = 0.36$  MPa), (b) Hysteretic curve in case of partial slip and total sliding (pre-load  $N_0 = 0.09$  MPa).

and some do not. The partial slip regime is the case where our previously developed Method of Memory Diagrams (MMD) can be applied, which allows one to get a tangential load-displacement relationship for any possible loading history. A straightforward extension of the MMD algorithm also allows to obtain the exact solution in case of two other contact regimes: contact loss and total sliding. Finally, the calculated load-displacement relations are used as an internal boundary condition defined at the crack boundaries in the wave propagation model, that is implemented in COMSOL Multiphysics<sup>®</sup>. The full numerical tool can be applied as modeling support for modern nonlinear acoustic NDT methods, as illustrated in this communication, but can also be of interest for researchers dealing with vibrations of loaded contacts, nonlinear metamaterials, thermography, etc.

## References

- [1] J. Krautkramer, H. Krautkramer, Ultrasonic testing of materials, Springer, 1990.
- [2] I. Solodov, N. Krohn, G. Busse, CAN: an example of nonclassical acoustic nonlinearity in solids, *Ultrasonics* 40 (2002) 621–625.
- [3] K. Van Den Abeele, P. Johnson, A. Sutin, Nonlinear elastic wave spectroscopy (NEWS) techniques to discern material damage, Part I: Nonlinear wave modulation spectroscopy (NWMS), *Res. Nondestruct. Eval.* 12 (2000) 17–30.
- [4] K. Van Den Abeele, J. Carmeliet, J. Ten Cate, P. Johnson, Nonlinear elastic wave spectroscopy (NEWS) techniques to discern material damage, Part II: Single-mode nonlinear resonance acoustic spectroscopy, *Res. Nondestruct. Eval.* 12 (2000) 31–42.
- [5] C. Pecorari, I. Solodov, *Universality of nonclassical nonlinearity: applications to non-destructive evaluation and ultrasonics*, Springer, 2007, Ch. Nonclassical nonlinear dynamic of solid surfaces in partial contact for NDE applications, pp. 309–326.
- [6] D. Broda, W. Staszewski, A. Martowicz, T. Uhl, V. Silberschmidt, Modelling of nonlinear crack-wave interaction for damage detection based on ultrasound - A review, *Journal of Sound and Vibration* 333 (2014) 1097–1118.
- [7] COMSOL AB, Stockholm, Sweden, COMSOL Multiphysics<sup>®</sup> v. 5.2.  
URL [www.comsol.com](http://www.comsol.com)

- [8] COMSOL AB, Stockholm, Sweden, LiveLink™ for MATLAB®, User's Guide, COMSOL Multiphysics® v. 5.2 (2015).
- [9] V. Aleshin, O. Bou Matar, K. Van Den Abeele, Method of memory diagrams for mechanical frictional contacts subject to arbitrary 2D loading, *Int. J. Solids Struct.* 60-61 (2015) 84–95.
- [10] S. Biwa, S. Nakajima, N. Ohno, On the acoustic nonlinearity of solid-solid contact with pressure-dependent interface stiffness, *Journal of Applied Mechanics* 71 (4) (2004) 508–515.